Polymer 51 (2010) 3123–3129

Contents lists available at ScienceDirect

Polymer

journal homepage: www.elsevier.com/locate/polymer

Fluorine-containing arborescent polystyrene-*graft*-polyisoprene copolymers as polymer processing additives

Mario Gauthier [a,*], Wai-Yau Lin [a], Steven J. Teertstra [a], Costas Tzoganakis [b]

[a] Institute for Polymer Research, Department of Chemistry, University of Waterloo, Waterloo, Ontario N2L 3G1, Canada
[b] Department of Chemical Engineering, University of Waterloo, Waterloo, Ontario N2L 3G1, Canada

ARTICLE INFO

Article history:
Received 4 February 2010
Received in revised form
19 April 2010
Accepted 20 April 2010
Available online 28 April 2010

Keywords:
Dendritic graft polymers
Polymer processing additives
Melt extrusion defects

ABSTRACT

Linear low density polyethylene (LLDPE) can suffer from melt extrusion defects including sharkskin, cyclic melt fracture, and gross melt fracture during processing. Arborescent polymers are dendritic macromolecules with characteristics, such as a compact structure and a rigid spherical topology, making them potentially useful as polymer processing additives (PPA) to alleviate melt extrusion defects. Arborescent polystyrene-*graft*-polyisoprene copolymer samples were synthesized from polystyrene substrates of linear and branched architectures functionalized with acetyl groups, and coupled with polyisoprene macroanions. A linear polyisoprene sample was also investigated for comparison. The polymers were hydrosilylated with (tridecafluoro-1,1,2,2-tetrahydrooctyl)dimethylsilane on 17–52% of the isoprene units and blended with LLDPE at 0.1 and 0.5% w/w to evaluate their performance as PPA by extrusion at different shear rates. All the samples led to some degree of improvement in the extrusion of LLDPE, albeit the performance of the branched additives was inferior to a commercial fluoroelastomer PPA. The lower molecular weight and more compact (G0 or comb-branched) PPA generally performed better than those with a high molecular weight. Several PPA samples induced the early onset of cyclic melt fracture but glossy, defect-free surfaces were obtained at higher shear rates. This suggests that a minimum shear rate is required for these additives to coat the extrusion die under the experimental conditions used.

1. Introduction

Melt extrusion defects such as sharkskin (SS), cyclic melt fracture (CMF), and gross melt fracture can be observed in the processing of different commodity polymers including linear low density polyethylene (LLDPE) and high density polyethylene (HDPE). Among these defects, SS is most problematic because it can occur even at low processing rates. The origin of SS is still under debate, however it is widely accepted that it forms when the polymer exits the die [1,2].

Additives are used to eliminate SS and delay the onset of CMF. These are most commonly fluoroelastomers, also known as polymer processing additives (PPA). The PPA are blended with the host polymer at a low concentration, typically 1000 ppm or 0.1% w/w [3]. The PPA migrate from the polymer melt to the die wall during processing and form a stagnant layer acting as lubricant for the host polymer, hence allowing it to slip on the die [4,5]. An effective PPA is generally immiscible with the host polymer, which facilitates its migration to the die wall [6,7], and has no detrimental effects on the mechanical (tensile) properties of the matrix polymer at low concentrations [8].

A new class of additives based on dendritic polymers was investigated over the last 20 years. Hyperbranched polymers are dendritic molecules with a high branching density and a very irregular structure (Fig. 1a), obtained in a one-pot synthesis from multifunctional monomers [9,10]. It was first shown by Kim and Webster that hyperbranched polyphenylene, when blended with polystyrene at 5% w/w, reduced its melt viscosity by 50% at 190 °C [11]. Similar effects were reported subsequently by Mulkern and Beck Tan for blends of polystyrene and a hyperbranched polyol [12]. Hong et al. also demonstrated that SS formation in the extrusion of LLDPE blended with Boltorn® hyperbranched polyester at 0.05–0.1% w/w was reduced, and completely eliminated at higher concentrations (0.5–1.0% w/w) [13]. The same blends yielded similar results in film blowing operations [14]. Finally, decreases in mixing torque reaching up to 15% were reported in the melt mixing of a hyperbranched polyester at 0.05–0.5% w/w with polypropylene [15].

* Corresponding author. Tel.: +1 519 888 4567; fax: +1 519 746 0435.
E-mail address: gauthier@uwaterloo.ca (M. Gauthier).

0032-3861/$ – see front matter © 2010 Elsevier Ltd. All rights reserved.
doi:10.1016/j.polymer.2010.04.044

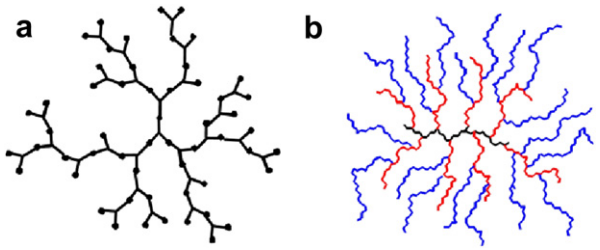

Fig. 1. Structure comparison for (a) hyperbranched and (b) arborescent polymers.

Arborescent polymers are another family of dendritic macromolecules with randomly distributed branching points (Fig. 1b), but obtained in a generation-based scheme where living polymer chains are grafted onto suitably functionalized polymer substrates. Very high molecular weights are thus attained in a few grafting cycles. This procedure provides molecules with a relatively well-defined structure as compared to hyperbranched polymers (Fig. 1). The arborescent molecules are very compact [16,17] and behave like rigid spheres, in contrast to linear and hyperbranched polymers. The application of arborescent polymers as PPA is relatively unexplored, but the analogous structures of hyperbranched and arborescent polymers suggest that the latter could also be useful for these applications. Furthermore, very recent modeling studies predicted that highly branched polymers possessing a high symmetry (e.g. star-branched polymers with a high branching functionality, and by extension arborescent polymers) would be best suited as PPA among branched polymer architectures, due to their greater tendency to diffuse to the surface of polymer blends [18]. Khadir and Gauthier indeed attributed the decreases in melt viscosity observed in blends of arborescent polystyrene and linear poly(methyl methacrylate) to the migration of the arborescent polymer to the surface of the polymer melt, albeit the arborescent polymer concentrations used in the investigation were relatively high (5–10% w/w) [19]. The introduction of fluorinated segments in the arborescent molecules should further enhance phase separation from the host polymer and make these materials more effective as PPA at low concentrations.

To explore the potential of fluorine-containing arborescent molecules as PPA at low concentrations (0.1–0.5% w/w), arborescent polystyrene-*graft*-polyisoprene copolymers were synthesized with variations in structure (branching functionality, side chain molecular weight) and composition (fluorine content). The samples served to correlate the characteristics of the molecules with their performance, evaluated by blending with LLDPE and extrusion, to focus on their ability to alleviate sharkskin formation and delay melt fracture.

2. Experimental procedures

Detailed procedures for the synthesis of arborescent copolymers by grafting polyisoprene (PIP) side chains onto acetylated polystyrene (PS) substrates have been described elsewhere [20]. Only the procedures significantly modified are described here.

2.1. Synthesis of arborescent polystyrene-graft-polyisoprene

Acetylated linear and generation zero (G0 or comb-branched) polystyrenes (G0PS) served as substrates for the grafting reaction. The G0PS sample was synthesized from a linear polystyrene substrate and side chains with a weight-average molecular weight $M_w \approx 5000$. The linear and G0PS substrates were acetylated to 30 and 33 mol%, respectively. Polyisoprenyllithium was synthesized by living anionic polymerization in tetrahydrofuran (THF) at −20 °C for 30 min, at 0 °C for 30 min, and lastly at 23 °C for 30 min, to yield a mixed chain microstructure [21]. The M_w of the PIP side chains varied from ca. 6000–45,000.

Linear PIP samples with $M_w = 3.16 \times 10^4$ and 1.15×10^5 were also synthesized under the same conditions.

2.2. Synthesis of (tridecafluoro-1,1,2,2-tetrahydrooctyl) dimethylhydrosilane

The procedure for the synthesis of the fluorohydrosilane (FHS) was adapted from the methods described by Ojima et al. [22] and Hwang et al. [23]. 1H,1H,2H-Perfluoro-1-octene (130.0 g, 0.376 mol) and Wilkinson's catalyst (0.296 g, 0.320 mmol) were loaded into a 250 mL high pressure flask with a magnetic stirring bar. Excess chlorodimethylsilane (50 g, 0.528 mol) was added with THF (25 mL) to the flask, which was sealed with a threaded poly(tetrafluoroethylene) stopper and heated to 120 °C for 48 h while stirring. Complete conversion of the octene to the fluorinated chlorosilane was confirmed by ^{1}H NMR analysis. The sample was distilled under reduced pressure (yield 150.3 g, 91%). The recovered chlorosilane was reduced with $LiAlH_4$ (30.4 g, 0.803 mol) in 500 mL of THF with stirring for 24 h. Complete reduction of the chlorosilane to (tridecafluoro-1,1,2,2-tetrahydrooctyl)dimethylhydrosilane was confirmed by ^{1}H NMR analysis. The FHS was distilled under reduced pressure (20 mm Hg at 60 °C; yield 150.3 g, 91%), stirred over CaH_2 for 48 h, and distilled again under reduced pressure (yield 90.6 g, 92%). The purity of the FHS was confirmed by ^{1}H NMR spectroscopy analysis [0.45 ppm (doublet), 1.15 ppm (multiplet), 2.19 ppm (septet), 3.95 ppm (septet)].

2.3. Hydrosilylation

The double bonds of PIP were functionalized with FHS via hydrosilylation by adapting a procedure reported for the hydrosilylation of polybutadiene [24]. The reaction provided as an example uses sample G0PS-PIP45 ($M_w = 7.92 \times 10^6$, PDI = 1.10) as a substrate. The copolymer (1.6 g, 23.5 meq isoprene units) was loaded in a 250 mL round bottom flask with a magnetic stirring bar, dried under vacuum for 48 h, and dissolved in 100 mL of dry cyclohexane under nitrogen after sealing the flask with a rubber septum. After dissolution of the copolymer, FHS (4.35 g, 10.5 mmol) and 0.3 mL of Karstedt catalyst were added with stirring. The reaction was terminated with methanol when the desired substitution level was attained (as determined by ^{1}H NMR analysis), when there was no further increase in the substitution level, or when the copolymer precipitated out of solution. The sample was precipitated in a solution of 10% v/v acetone in methanol, and further purified by three cycles of dissolution in THF and precipitation in methanol. The functionalized polymer was finally dried under vacuum and the hydrosilylation level was determined by ^{1}H NMR analysis.

2.4. Characterization

The absolute molecular weight of the polystyrene substrates, the copolymers, the PIP side chains, and the linear PIP samples was determined on a Viscotek TDA 302 gel permeation chromatography (GPC) instrument equipped with a light scattering detector. The system included a Waters AF inline degasser, a Waters 515 HPLC pump, a 717plus auto sampler, a 50 × 7.5 mm^2 Polymer Laboratories gel 10 μm guard column, and three PLgel 10 μm mixed-B columns (300 × 7.5 mm^2) covering a molecular weight range of 5×10^2–1×10^7. The system utilized a Viscotek TDA 302 Triple detector with right-angle (RALS) and low-angle light scattering (LALS) detectors operating at 670 nm, as well as DRI and viscometer

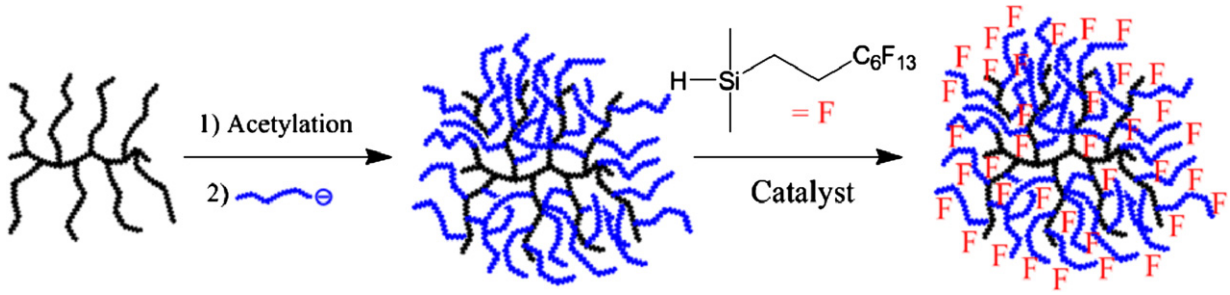

Scheme 1. Synthesis of a G1 arborescent copolymer PPA.

detectors. A UV detector (model 2501) was also incorporated as an add-on. The molecular weight distribution of the samples was calculated with the OmniSEC v3.0 software package from Viscotek. Refractive index increment (d*n*/d*c*) measurements were conducted on a Brice-Phoenix differential refractometer equipped with a 632 nm band-pass interference filter.

The microstructure of the PIP samples and the composition of the copolymers were analyzed by ^{1}H NMR spectroscopy on a Bruker AC-300 nuclear magnetic resonance spectrometer in $CDCl_3$ at a concentration of ca. 10 mg/mL. The method used to determine the microstructure of the PIP side chains was described by Essel and Pham [21].

The glass transition temperature (T_g) of a linear PIP mixed microstructure sample with M_w = 31,600 (PIP32) before and after FHS modification on 49% of the isoprene units (PIP32-F49) was measured with a TA Instruments Differential Scanning Calorimeter (DSC) model Q100 equipped with a refrigerated cooling system, using the TA Instruments Universal Analysis 2000 software package. The samples (~10 mg) were dried under vacuum for two days and sealed in aluminum pans for the measurements. Each sample was equilibrated at −90 °C and scanned at a rate of 10 °C/min up to 120 °C. Duplicate scans were collected in the same temperature range to ensure reproducibility of results. The T_g values reported correspond to the mid-point change in heat capacity in the transition region, and were reproducible to within ±0.2 °C for successive scans.

Atomic force microscopy (AFM) characterization of films prepared from unmodified and fluorinated arborescent isoprene copolymers was carried out using a Multimode Nanoscope IIIa instrument, Veeco Inc., Santa Babara, CA. The copolymers were dissolved in heptane at a concentration of 0.25–0.65 mg/mL. Monomolecular films were obtained by spin-casting of the solutions onto mica (spinning rate 3000 rpm). The AFM measurements were done at room temperature (25 °C) and a relative humidity of 30–40%, in the tapping mode using a silicon cantilever with a spring constant of 50 N/m and a resonance frequency of 160 kHz.

2.5. Blending of the PPA with LLDPE

A commercial LLDPE resin (LL1001.32, Exxon Mobil Chemical) with 2% w/w butene comonomer content, stabilized with 0.03% w/w of octadecyl-3-(3,5-di-*tert*-butyl-4-hydroxyphenyl) propionate, having a melt flow index of 1.0 g/10 min (ASTM D1238), was used in the investigation.

The following procedure describes the preparation of a blend with the PPA (fluorinated copolymer). A master batch was obtained by compounding LLDPE resin (198 g) with 2.0 g of additive (for a concentration of 1.0% w/w) in a Haake Rheocord 90 batch mixer with a Rheomix 3000 mixing chamber at 190 °C (5 min at 50 rpm). The copolymer master batches were then diluted to 0.5% w/w with virgin LLDPE, by compounding 100 g of the master batch and 100 g of virgin LLDPE. Two samples (G0PS-PIP6-F17 and PS-PIP6-F25) were selected for further testing at a final PPA concentration of 0.1% w/w, by compounding 40 g of the copolymer blends at 0.5% w/w and 160 g of LLDPE. With the exception of the master batch, all the samples were ground into flakes.

2.6. Extrusion testing

Testing of the samples was conducted on a Kayeness Galaxy V capillary rheometer (Model 8052) equipped with a stainless steel die (0.02″ diameter, L/D = 50, entrance angle = 90°). All the extrusion operations were done at 190 °C. The die was cleaned by extruding LLDPE containing 50% w/w of $CaCO_3$, and then virgin LLDPE to remove PPA residues in-between runs. Pure LLDPE was extruded as baseline control and the extrudate was examined to ensure that the sample was not affected by additives used in the previous run (i.e. no residual glossiness at a shear rate of 300 s^{-1}). The die was coated with the sample at a shear rate of 300 s^{-1} until a constant load (backpressure) was achieved. The blends were tested at shear rates from 50 to 1000 s^{-1} until a constant load was achieved at each shear rate.

2.7. Optical microscope study of droplet size

The droplet size study was adapted from a procedure developed for the analysis of the Dynamar® additive (FX9613) dispersed in polyolefins [25]. Four to six flakes of the ground sample were placed between two 2.5 × 7.5 cm^2 microscope glass slides heated on a hot plate at ca. 150 °C for 5 min and a 4 kg weight was put on the slides to create a thin film (ca. 200 μm). The slides were examined on a Radical RXL-4B optical microscope at room temperature, at a magnification of 100×. The microscope was equipped with an AmScope 640 × 480 digital camera and calibrated using a 1.0 mm ABBOTA stage micrometer slide with 10 μm divisions. The diameter of the additive droplets was measured using the AmScope 3.0 software provided with the instrument. At least 10 measurements were used to calculate the average and standard deviation on the droplet diameters.

3. Results and discussion

The synthesis of a generation one (G1) arborescent PPA by grafting polyisoprene side chains onto an acetylated G0 polystyrene substrate and chemical modification with the FHS via hydrosilylation is depicted in Scheme 1. Each step of the reaction will be discussed in further details below.

3.1. Polystyrene substrates characterization

The characteristics of the polystyrene grafting substrates were determined by GPC analysis with DRI and light scattering (RALS and LALS) detectors before acetylation, and by ^{1}H NMR spectroscopy after the acetylation reaction (Table 1). The acetylation level was set

Table 1
Polystyrene substrates used in the synthesis of the graft copolymers.

Polymer	M_w^{sc} [a]	M_w/M_w^{sc} [a]	M_w [b]	f_w	$-COCH_3$ mol% [c]	Coupling sites
PS (linear)	6500	1.08	–	–	30	19
G0PS	5800	1.07	1.04×10^5	17	33	330

[a] Absolute values for the side chains determined by GPC analysis with DRI detector.
[b] Absolute M_w determined by GPC analysis with RALS and LALS detectors.
[c] Acetylation level from ^{1}H NMR analysis.

at around 30 mol%. The weight-average branching functionality of the G0 substrate and the PIP copolymers, f_w, corresponding to the number of chains added in the last grafting reaction, was calculated from Equation (1), where $M_w(G)$, $M_w(G-1)$, and M_w^{sc} are the absolute weight-average molecular weight of graft polymers of generation G, of the preceding generation, and the added side chains, respectively. The number of coupling sites on the substrates was calculated from their absolute M_w and acetylation level.

$$f_w = \frac{M_w(G) - M_w(G-1)}{M_w^{sc}} \quad (1)$$

3.2. Arborescent polystyrene-graft-polyisoprene

The nomenclature used for the copolymers indentifies the structure (generation number) of the substrate, and the molecular weight of the grafted side chains. For example, G0PS-PIP45 corresponds to a copolymer structure of overall generation G1, derived from a G0PS substrate and PIP side chains with M_w = 45,000. The absolute molecular weight and polydispersity index of each isoprene copolymer sample synthesized (Table 2) was determined by GPC analysis. The low polydispersity indices (PDI = 1.01–1.10) found for all the graft copolymer samples are indicative of a uniform distribution of side chains among the molecules. The coupling efficiency C_e, corresponding to the percentage of coupling sites consumed in the grafting reaction, was calculated as the ratio of f_w to the total number of coupling sites on the substrate. The coupling efficiency is lower for the G0 than for the linear substrate, and declines as the molecular weight of the PIP side chains increases. These variations in coupling efficiency were observed previously [17] and attributed to steric (excluded volume) effects limiting the accessibility of the coupling sites as the number and the size of the chains grafted on the substrate is increased.

3.3. Hydrosilylation

Both the linear PIP and arborescent copolymer samples were modified with the FHS through hydrosilylation. The characteristics of the FHS-substituted polymers are summarized in Table 3. The nomenclature used for the fluorinated derivatives is analogous to the parent copolymers, but also specifies the substitution level attained. For example, G0PS-PIP45-F39 corresponds to a copolymer having 39% of the isoprene units modified with FHS. The substitution level was controlled through the amount of FHS added and the reaction time, and was monitored by ^{1}H NMR spectroscopy (Fig. 2). The peaks for the silylmethyl group (ca. 0 ppm) and the olefinic protons (4.5–6 ppm) were used to quantify the substitution level, ranging from 17 to 52 mol%.

Apparent (polystyrene-equivalent) molecular weights and PDI values are also reported for the fluorinated polymers in Table 3. High molecular weight samples having substitution levels above 39 mol% were insoluble in THF and could not be characterized by GPC analysis. The apparent PDI of the samples remained low after hydrosilylation (PDI < 1.2 for most samples), indicating the absence of side reaction during the hydrosilylation process. Samples G0PS-PIP45-F19 and G0PS-PIP45-F28 have PDI values of 1.33 and 1.54 respectively, however. The increase in PDI could be due either to slight cross-linking of the polymers, or else to difficulties in GPC analysis of the sample (e.g. adsorption on the columns).

The residual microstructure of isoprene units in the FHS-substituted homo and copolymers was analyzed by ^{1}H NMR spectroscopy. Detailed analysis of the ^{1}H NMR spectra (Fig. 2c and Table 3) shows that the 1,2-units are more reactive towards hydrosilylation than the 1,4- and 3,4-units. A significant fraction of 1,4-units nonetheless reacted under the conditions used, but overlap of the peaks for the *cis* and *trans* units does not allow resolution of the two 1,4-isomers. The relative reactivity of the three types of isoprene units therefore follows the trend 1,2- > 1,4- >> 3,4-. Two of the samples (PS-PIP6-F25, and G0PS-PIP6-F17) do not follow the same trend, however. The reactivity of the 1,2- and 1,4-units in these samples appears similar, with no preference for the 1,2- or the 1,4-units in the hydrosilylation reaction. This effect could be related to the presence of impurities in the reaction, but the exact cause still needs to be eluded. One area of commonality between the three samples is that they have low FHS substitution.

DSC analysis of the linear mixed microstructure PIP32 substrate and the fluorinated polymer PIP32-F49 was performed to investigate the influence of the FHS substituent on the thermal properties of the polymer. The glass transition temperature (T_g) of the linear PIP32 substrate was -15.8 ± 0.2 °C, and the change in heat capacity

Table 2
Characteristics of the linear PIP and arborescent polystyrene-*graft*-polyisoprene copolymers synthesized.

Polymer	Side chains				Linear PIP/Arborescent copolymer				C_e, % [c]
	M_w [a]	1,2-PIP mol%	1,4-PIP mol%	3,4-PIP mol%	M_w [a]	PDI M_w/M_n [a]	PIP % w/w [b]	f_w	
PIP32 [d]	–	31	33	36	3.16×10^4	1.08	–	–	–
PIP115	–	33	34	33	1.15×10^5	1.05	–	–	–
PS-PIP6	6500	28	35	37	1.39×10^5	1.01	95	19	100
PS-PIP28	28,000	31	33	36	3.96×10^5	1.10 [b]	99	14	73
G0PS-PIP6	6000	31	37	32	1.83×10^6	1.01	94	283	86
G0PS-PIP13	13,000	34	34	33	3.40×10^6	1.05	97	248	75
G0PS-PIP24	24,100	33	36	30	5.06×10^6	1.02	98	206	62
G0PS-PIP45	44,600	31	40	29	7.92×10^6	1.10	99	177	54

[a] Absolute values determined with the RALS/LALS detectors. $M_w/M_n \leq 1.10$ for the side chains.
[b] Polyisoprene content estimated from the absolute M_w of the substrate and the graft copolymer.
[c] Coupling efficiency.
[d] Sample nomenclature: PIPXXX linear PIP, XXX = molecular weight/10^3; PS-PIPXX and G0PS-PIPXX graft copolymers.

Table 3
FHS modification of linear and arborescent PIP copolymers.

Polymer[a]	M_w^{app}[b]	M_w/M_n^{app}[b]	M_w^{abs}[c]	Residual microstructure		
				1,2-PIP	1,4-PIP	3,4-PIP
PIP32-F49	3.20×10^4	1.08	1.17×10^5	0	28	72
PIP115-F26	1.16×10^5	1.18	2.92×10^5	11	33	56
PIP115-F42	Insol	Insol	4.02×10^5	0	30	70
PS-PIP6-F25	5.83×10^4	1.08	3.23×10^5	25	20	55
PS-PIP6-F41	Insol	Insol	4.41×10^5	0	44	56
PS-PIP6-F50	Insol	Insol	5.07×10^5	0	42	58
PS-PIP28-F44	1.60×10^5	1.06	1.42×10^6	0	31	69
G0PS-PIP6-F17	2.33×10^5	1.13	3.55×10^6	31	32	37
G0PS-PIP6-F22	1.70×10^5	1.08	4.06×10^6	19	34	47
G0PS-PIP6-F27	2.69×10^5	1.14	4.56×10^6	22	32	46
G0PS-PIP6-F42	Insol	Insol	6.08×10^6	0	41	59
G0PS-PIP6-F52	Insol	Insol	7.09×10^6	0	34	66
G0PS-PIP13-F31	1.09×10^5	1.08	9.35×10^6	21	28	51
G0PS-PIP13-F41	Insol	Insol	1.13×10^7	0	42	58
G0PS-PIP24-F25	5.36×10^5	1.19	1.25×10^7	18	31	51
G0PS-PIP24-F39	Insol	Insol	1.66×10^7	6	17	77
G0PS-PIP45-F19	5.49×10^5	1.33	1.69×10^7	25	34	41
G0PS-PIP45-F28	5.56×10^5	1.54	2.11×10^7	14	37	49
G0PS-PIP45-F39	Insol	Insol	2.63×10^7	4	32	64

[a] Sample nomenclature as in Table 2, substitution level (mol%) determined by ^{1}H NMR spectroscopy indicated as -FXX.
[b] Apparent values determined using GPC calibrated with linear polystyrene.
[c] Absolute M_w calculated from fluorine content (^{1}H NMR) and absolute M_w of substrate.

(ΔC_p) for the transition was 0.36 ± 0.3 J g^{-1} K^{-1}. The attachment of the PHS at 49% of the isoprene units led only to a small increase in T_g (-14.3 ± 0.3 °C), but the transition broadened and ΔC_p decreased significantly (0.23 ± 0.3 J g^{-1} K^{-1}). Since the glass transition temperature and the resulting step increase in heat capacity is generally attributed to the onset of crankshaft (Schatzki) motions in polymer chains, the small ΔC_p value for the fluorinated polymer may reflect a decrease in mobility for the PIP chains upon attachment of the PHS to nearly half of the isoprene units. No additional transitions were observed in the DSC traces from −80 to 80 °C for the fluorinated polymer, indicating that the PHS-modified linear PIP is completely amorphous.

Atomic force microscopy was used to observe the topology of monomolecular films of selected arborescent isoprene copolymer substrates and fluorinated copolymers on mica. The films were investigated in the tapping mode, using both height and phase imaging, and yielded clearly resolved images (Fig. 3). The copolymers were observed as close-packed monolayers of molecules, both before and after attachment of FHS, further confirming the absence of side reactions during hydrosilylation. For films cast from heptane, a solvent selective for PIP, good phase contrast was observed between the polystyrene core and the PIP side chains in the phase mode. The images for G1 copolymers with long PIP arms ($M_w \approx 24{,}000$) contain lighter domains attributed to the harder polystyrene-rich core dispersed in the softer PIP matrix formed by the side chains, providing direct evidence for retention of a core-shell morphology after hydrosilylation.

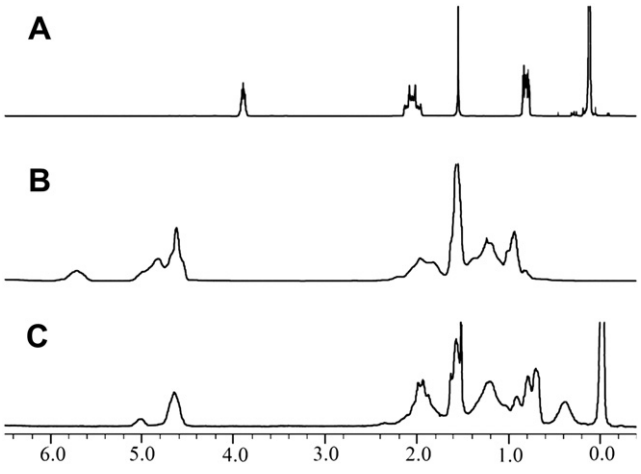

Fig. 2. ^{1}H NMR spectra for (A) the FHS, (B) copolymer PS-PIP6, and (C) the fluorinated polymer (PS-PIP6-F41).

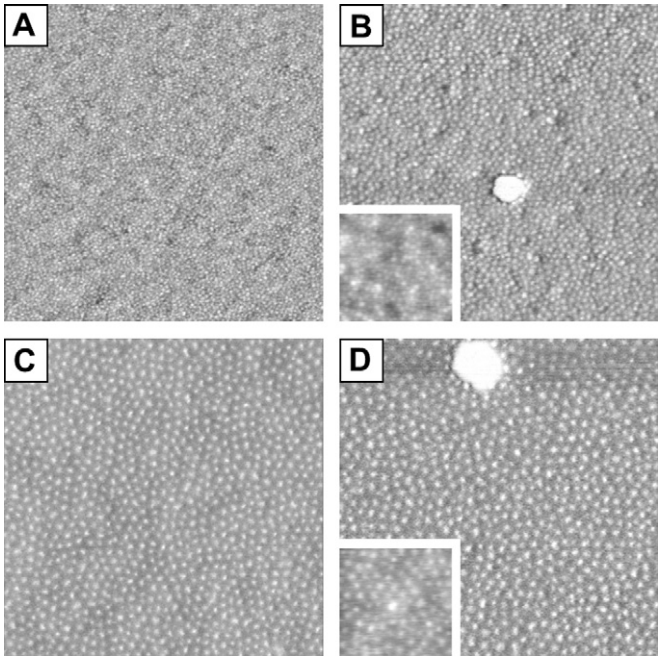

Fig. 3. AFM images of samples prepared on mica by spin-casting from heptane solutions: (A) G0PS-PIP6, (B) G0PS-PIP6-F52, (C) G0PS-PIP24, and (D) G0PS-PIP24-F25. The images are shown in the phase contrast mode and have a width of 1 μm. The insets in (B) and (D) are height images showing the topology of the monolayers.

Table 4
Extrusion of commercial additive and FHS-substituted polymer blends at 0.5% w/w.

Sample	Pressure reduction, %[a]				Extrudate appearance[b]
	50 s^{-1}	100 s^{-1}	200 s^{-1}	300 s^{-1}	
FX9613	64.8	69.2	65.9	60.3	Glossy@50–1000 s^{-1}
PIP115-F26	7.5	5.9	4.0	3.4	CMF@ ≥400 s^{-1}
PIP115-F42	9.4	8.4	6.6	–	CMF@ ≥300 s^{-1}
PS-PIP6-F25	11.8	–	–	28.7	Mild CMF@ 100 s^{-1} Glossy@ 300-400 s^{-1}
PS-PIP6-F41	8.6	–	–	–	CMF@ ≥100 s^{-1}
PS-PIP6-F50	7.3	–	–	–	Mild CMF@ 100 s^{-1}
PS-PIP28-F44	1.7	3.0	–	–	CMF@ ≥200 s^{-1}
G0PS-PIP6-F17	9.2	6.4	–	20.3	Glossy @ 300-400 s^{-1}
G0PS-PIP6-F22	3.1	3.6	3.12	3.0	SS@ 200-400 s^{-1}
G0PS-PIP6-F27	9.0	–	–	–	Mild CMF@ 100 s^{-1}
G0PS-PIP6-F42	12.0	10.4	–	–	CMF@ ≥200 s^{-1}
G0PS-PIP6-F52	5.4	7.2	–	–	Glossy@ 400-600 s^{-1}
G0PS-PIP13-F31	8.0	–	–	–	Mild CMF@ 100 s^{-1}
G0PS-PIP13-F41	11.8	9.2	–	–	CMF@ ≥200 s^{-1}
G0PS-PIP24-F25	8.22	7.6	–	–	CMF@ ≥200 s^{-1}
G0PS-PIP24-F39	7.46	7.5	–	–	CMF@ ≥200 s^{-1}
G0PS-PIP45-F19	4.4	3.4	–	9.2	Glossy@ 300-400 s^{-1}
G0PS-PIP45-F28	4.4	6.0	4.5	–	CMF@ ≥300 s^{-1}
G0PS-PIP45-F39	7.5	7.2	5.8	–	SS@ 200 s^{-1}

[a] Percent reduction as compared to pure LLDPE; '–' indicates that CMF was observed.
[b] Pure LLDPE displays SS at 200–300 s^{-1} and normal CMF at 400 s^{-1}.

3.4. Extrusion with linear and arborescent PPA at 0.5% w/w concentration

The results obtained for the extrusion of the FHS-substituted copolymers blended with commercial LLDPE at a concentration of 0.5% w/w are summarized in Table 4. Several of the PPA samples (PS-PIP6-F25, PS-PIP6-F50, G0PS-PIP6-F27, and G0PS-PIP13-F31) led to a mild form of CMF, characterized by alternating glossy and dull surfaces on the extrudate (Fig. 4). The dull surface is clearly rougher than the glossy surface, but not nearly as serious as in the case of SS formation. Furthermore, it is interesting to note that mild CMF occurred at very low shear rates (100 s^{-1}) and was immediately followed by normal CMF as the shear rate was increased. No pressure reductions are reported in Table 4 when CMF occurred, as the load oscillated between two values that were usually several hundred lbs apart under these conditions. In some cases (PS-PIP6-F25, G0PS-PIP6-F17, G0PS-PIP6-F52, G0PS-PIP45-F19) the onset of CMF was observed at low shear rates but it was eliminated afterwards, which suggests that these samples require a minimum shear rate to coat the die under the experimental conditions used. CMF formation eventually returned as the shear rate was increased due to the gradual load buildup. It has been demonstrated [6] that the time required for linear fluoroelastomer PPA to form a stable coating on the die wall (leading to melt defect elimination) varies with the shear rate, but that the extent of die coating is mainly determined by the volume of PPA extruded though the die rather than by the shear rate itself. It is clear that the flow rate of molten polymer increases with the shear rate used in the experiment, so that the die is coated more rapidly at higher shear rates. As the shear rate is further increased, the PPA layer is of course eventually stripped off the die wall and melt defects reappear. It has been predicted by modeling investigations and verified experimentally for some systems that the PPA concentration near the wall surface should be depleted, while experimental results have actually shown that for dendritic polymer additives, migration of the branched polymers to the wall is favored as the shear rate is increased [26]. This could explain the apparent "minimum" shear rate for die coating observed for some of the branched PPA samples (PS-PIP6-F25, G0PS-PIP6-F17, G0PS-PIP6-F52, G0PS-PIP45-F19) in the current investigation, although it is unclear why this effect is limited to these samples.

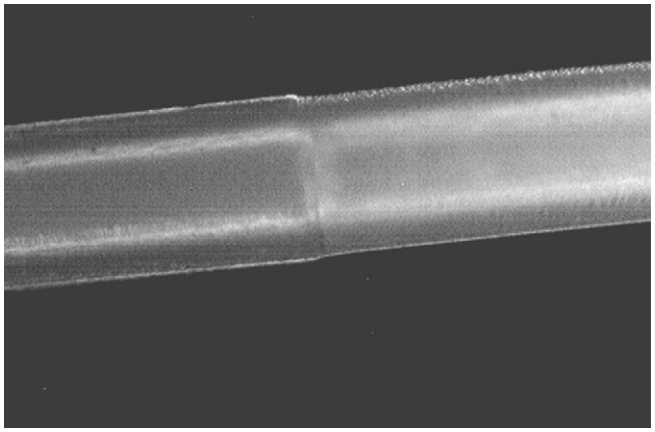

Fig. 4. Mild CMF observed for a 0.5% w/w blend of PPA with LLDPE extruded at a shear rate of 100 s^{-1}. Mild CMF appears as alternating blocks of glossy (left) and dull (right) surfaces (filament diameter 0.58 mm).

Table 5
Extrusion of commercial additive and selected FHS-substituted polymer blends at 0.1% w/w.

Sample	Pressure reduction[a,b] (%)				Extrudate appearance[c]
	50 s^{-1}	100 s^{-1}	200 s^{-1}	300 s^{-1}	
FX9613	43.8	56.4	57.3	53.7	Glossy@ 50-800 s^{-1}; CMF@ ≥1000 s^{-1}
PS-PIP6-F25	9.2	7.4	–	–	CMF@ ≥200 s^{-1}
G0PS-PIP6-F17	3.1	2.4	1.6	–	SS@ 200 s^{-1}, CMF@ ≥300 s^{-1}

[a] Percent reduction as compared to pure LLDPE.
[b] Experimental error limit for significant pressure reduction is ≈5%.
[c] Pure LLDPE displays SS at 200–300 s^{-1} and normal CMF at 400 s^{-1}.

When comparing the performance of the linear homopolymer (PIP115-F26, $M_w^{app} = 1.16 \times 10^5, M_w^{abs} = 2.92 \times 10^5$) with that of an arborescent copolymer PPA having a similar absolute molecular weight and fluorine content (PS-PIP6-F25, $M_w^{app} = 5.83 \times 10^4$, $M_w^{abs} = 3.23 \times 10^5$), it appears that the more compact branched sample (as demonstrated by its much lower apparent molecular weight) is more efficient at delaying the onset of melt fracture. This result is consistent with smaller molecules migrating more efficiently to the die wall during extrusion. The pressure reduction was much larger and the appearance of the extrudate remained glossy between 300 and 400 s^{-1} for the branched polymer, albeit a minimum shear rate was required for the formation of a stagnant coating.

The trends among the fluorinated polystyrene-*graft*-polyisoprene copolymer samples are not very clear. This is partly due to the difficulty in selecting the parameters (molecular weight, branching functionality, substitution level, etc.) serving as a basis for such a comparison. As the generation number of the copolymers increased from G0 to G1, the performance of the additives generally decreased. For example, PS-PIP6-F25 yielded a significant (12%) pressure reduction at 100 s^{-1} and the extrudate remained glossy up to 400 s^{-1}, but for G0PS-PIP6-F27 mild CMF started at 100 s^{-1} and normal CMF occurred immediately afterwards. Similar effects were also observed as the molecular weight of the grafted PIP chains was increased (e.g. G0PS-PIP6-F17 versus G0PS-PIP45-F19). All the PPA samples led to some backpressure reduction at the different shear rates investigated, but in many cases the reduction remained within the experimental error limits (estimated at ca. 5% in these types of measurements). When comparing samples with different

Table 6
Droplet size data for selected additives at 0.5% w/w and 0.1% w/w concentrations.

Sample	Concentration, % w/w	Diameter, μm (±)[a]
FX9613	0.5	1.38(0.29)
	0.1	1.38(0.34)
PS-PIP6-F25	0.5	1.58(0.42)
	0.1	2.08(0.47)
G0PS-PIP6-F17	0.5	1.40(0.37)
	0.1	1.50(0.31)

[a] Calculated standard deviation.

FHS substitution levels and the same M_w, it seems that substitution levels between 26 and 35 mol% are optimal.

A commercial PPA sample, FX9613, was also tested at a concentration of 0.5% w/w in LLDPE (Table 4). The commercial additive reduced the backpressure by 60–69% and completely eliminated SS. The onset of CMF was delayed to shear rates of 1100 s^{-1}.

3.5. Extrusion with linear and arborescent PPA at 0.1% w/w concentration

Two samples (PS-PIP6-F25, and G0PS-PIP6-F17) were selected on the basis of their good performance when extruded at 0.5% w/w to be evaluated at a low concentration (0.1% w/w) more typical of commercial PPA (Table 5). FX9613 was also tested at 0.1% w/w. As expected, the performance of all PPA was diminished when their concentration was decreased. For example, PS-PIP6-F25 eliminated SS formation and delayed CMF up to 400 s^{-1} at 0.5% w/w, but no processability improvement was observed at 0.1% w/w. While all samples suffered from melt defects, the reduction in backpressure still decreased in the order PS-PIP6-F25 > G0PS-PIP6-F17 at shear rates between 50 and 200 s^{-1}. This is again consistent with smaller molecules migrating more efficiently to the die wall during extrusion. The performance of FX9613 at 0.1% w/w was excellent in comparison with the PPA synthesized: This additive still eliminated SS, delayed the onset of CMF, and yielded a large reduction in backpressure at all shear rates. In comparison to the results obtained at 0.5% w/w, however, the magnitude of the backpressure reduction was decreased even for FX9613.

3.6. Droplet size

The average droplet size of PPA promoting the formation of a stable coating on the surface of the die was previously reported to be in the range of approximately 2 μm [27]. Contrary evidence have also arisen from other researchers suggesting that for an effective coating the droplet size should be greater than 2 μm [6,28,29].

The droplet size at 0.1% w/w and 0.5% w/w PPA concentration was determined through optical microscopy. The average droplet size and the standard deviation for each of samples blended with LLDPE are reported in Table 6. There are no significant size differences within the samples that were tested. Also, all samples have a droplet size that falls within a narrow range (1.38–2.08 μm). When comparing FX9613 droplets size with other samples, no trend could be seen as the droplet sizes are very similar. The decreased performance of the PPA is clearly unrelated to droplet size variations, as these are very similar at both concentrations.

4. Conclusions

Extrusion was conducted with arborescent polystyrene-*graft*-polyisoprene copolymers and linear polyisoprene functionalized with a fluorohydrosilane. The additives were evaluated when blended with LLDPE at 0.5% w/w. The effect of a lower additive concentration (0.1% w/w) was also investigated for PS-PIP6-F25 and G0PS-PIP6-F17. For comparison, a commercial additive (FX9613) was also tested at the same concentrations. The following conclusion can be drawn from the extrusion results:

1. Arborescent copolymer PPA blended at 0.5% w/w all reduced the backpressure during extrusion processing, although the reduction remains within experimental error limits in certain cases. The performance of the branched additives was inferior to that of a commercial fluoroelastomer PPA.
2. The lower molecular weight G0 copolymer PPA, having compact structures, were generally more effective than their higher molecular weight G1 counterparts. This effect could be related to enhanced diffusivity for the smaller G0 molecules.
3. Some samples required a minimum shear rate for effective coating of the die by the PPA under the experimental conditions used.
4. PS-PIP6-F25 and G0PS-PIP6-F17, when extruded at 0.1% w/w, yielded a significantly lower performance than at 0.5% w/w.
5. The droplet size of the PPA dispersed in LLDPE fell within a relatively narrow range between 1.03 μm and 2.07 μm, and was essentially independent of PPA concentration.

Acknowledgements

We acknowledge the financial support of the Natural Sciences Research Council of Canada (NSERC) and Imperial Oil Limited for the work. We thank Prof. Neil McManus for providing access to the GPC-LS equipment, and Prof. Sergei Sheiko for the AFM pictures of the arborescent polymers.

References

[1] Lenk RS. Plastics rheology – mechanical behaviour of solid and liquid polymers. New York: Wiley-Interscience; 1968. pp. 94–108.
[2] Brydson JA. Flow properties of polymer melts. New York: Van Nostrand Reinhold; 1970. pp. 78–81.
[3] Achilleos EC, Georgiou G, Hatzikiriakos SG. J Vinyl Additive Technol 2002;8:7–24.
[4] Migler KB, Lavallée C, Dillon MP, Woods SS, Gettinger CL. J Rheol 2001;45:565–81.
[5] Liu X, Li H. J Appl Polym Sci 2004;93:1546–52.
[6] Bigio D, Meillon MG, Kharchenko SB, Morgan D, Zhou H, Oriani SR, et al. J Nonnewton Fluid Mech 2005;131:22–31.
[7] Mackley MR, Rutgers RPG, Gilbert DG. J Nonnewton Fluid Mech 1998;76:281–97.
[8] Markarian JS. J Plastic Film Sheeting 2001;17:333–7.
[9] Malmström E, Hult A. In: Fréchet JMJ, Tomalia DA, editors. Dendrimers and other dendritic polymers. Chichester: Wiley; 2001. p. 197–208.
[10] Voit BI, Lederer A. Chem Rev 2009;109:5924–73.
[11] Kim YH, Webster OW. Macromolecules 1992;25:5561–72.
[12] Mulkern TJ, Beck Tan NC. Polymer 2000;41:3193–203.
[13] Hong Y, Cooper-White JJ, Mackay ME, Hawker CJ, Malmström E, Rehnberg N. J Rheol 1999;43:781–93.
[14] Hong Y, Coombs SJ, Cooper-White JJ, Mackay ME, Hawker CJ, Malmström E, et al. Polymer 2000;41:7705–13.
[15] Schmaljohann D, Pötschke P, Hässler R, Voit BI, Froehling PE, Mostert B, et al. Macromolecules 1999;32:6333–9.
[16] Gauthier M, Möller M. Macromolecules 1991;24:4548–53.
[17] Teertstra SJ, Gauthier M. Prog Polym Sci 2004;29:277–327.
[18] Qian Z, Minnikanti VS, Archer LA. J Polym Sci B Polym Phys 2008;46:1788–801.
[19] Khadir A, Gauthier M. Polym Mater Sci Eng 1997;77:174–5.
[20] Li J, Gauthier M. Macromolecules 2001;34:8918–24.
[21] Essel A, Pham QT. J Polym Sci Part A-1 1972;10:2793–801.
[22] Ojima I, Fuchikami T, Yatabe M. J Org Chem 1984;260:335–46.
[23] Hwang SS, Ober CK, Perutz S, Iyengar DR, Schneggenburger LA, Kramer EJ. Polymer 1995;36:1321–5.
[24] Hempenius MA, Michelberger W, Möller M. Macromolecules 1997;30:5602–5.
[25] Optical microscopy method for dispersion analysis in polyolefins. Dynamar Polymer Processing Additive Technical Information, Dyneon LLC; 2000.
[26] Kharchenko SB, McGuiggan PM, Migler KB. J Rheol 2003;47:1523–45 [and references cited therein].
[27] Amos SE, Giacoletto G, Horns J, Lavallée C, Woods S. In: Zweifel H, editor. Plastics additives handbook. Munich: Hanser Gardner; 2001. p. 553–84.
[28] Chapman Jr GR, Oriani SR. US Pat 6,642,310; 2003.
[29] Oriani SR. J Plastic Film Sheeting 2005;21:179–98.